A SUBSPACE APPROACH TO FAULT DIAGNOSTICS IN LARGE POWER SYSTEMS
(INVITED PAPER)

Romain Couillet[1] *and Enrico Zio*[1,2]

[1] *Centrale-Supélec-EDF Chair on System Sciences and the Energy Challenge, France.*
[2] *Department of Energy, Politecnico di Milano, Italy.*

ABSTRACT

In this article, a recently proposed subspace approach for diagnosing sudden local changes in large dynamical networks is applied to the detection and localization of link failures in power systems, on the basis of nodal voltage measurements.

I. INTRODUCTION

The future energy distribution networks will be characterized by increased dynamics due in particular to the progressive penetration of unreliable energy production sources into the grid. In order to maintain the grid stability, it is therefore compelling to keep regular observations of the system as a whole and to fast detect and identify possible failures. In this article, we focus on failures in power lines which translate in sudden changes in the electric impedance. To keep track of the current flowing in the line as well as the voltages at the nodal connections, it suffices to track impedance changes. However, while voltage measurements are available at any time, e.g. thanks to phasor measurement units (PMU), transmission line states are only refreshed on an hourly basis [1]. For rather static systems, the authors in [1] developed a phasor-based fault detection and localization technique, which identifies line failures among predetermined angle shift patterns. In the future smart grids, however, it is expected that the dynamics will make it difficult to isolate natural phase distortions from failures, and will require a continuous update of the predetermined failure angle patterns, which is impractical.

This article tackles this problem by first demonstrating that successive voltage observations of a line outage can be mathematically modeled by a *spiked sample covariance matrix* [2, Chapter 9]. Using a recent random matrix subspace method for local failure diagnosis in large sensor networks [3], we then provide an improved method for detecting and diagnosing link failures. The method is then tested on a benchmark IEEE-bus system.

The remainder of the article is structured as follows. In Section II, we introduce the model of the electrical system. In Section III, we recall relevant results from random matrix theory and introduce the novel failure diagnosis method. Simulation results are then provided in Section IV. Finally, Section V concludes this article.

II. ELECTRICAL NETWORK MODEL

II-A. Normal functioning: Hypothesis $\mathcal{H}_0$

Consider the voltages $V(t) = (V_1(t), \ldots, V_N(t))^\mathsf{T} \in \mathbb{C}^N$ in an N-node interconnected electricity network at time t. The power injection at node k (issued by the energy production unit connected to node k) is denoted $I_k(t)$ and satisfies $I_k(t) = \bar{I}_k + i_k(t)$ with $\bar{I}_k$ a known mean value and $i_k(t)$ a complex Gaussian fluctuation modeling both the time variations in the node input current flow (due to the stochasticity of renewable energy production) and the uniform distribution of the voltage angles under irregular sampling. We assume the $i_k(t)$ independent across k and, for simplicity, identically distributed circularly symmetric $\mathcal{CN}(0,1)$; we denote $\bar{I} = (\bar{I}_1, \ldots, \bar{I}_N)^\mathsf{T}$ and $i(t) = (i_1(t), \ldots, i_N(t))^\mathsf{T}$.[1]

From Kirchoff's laws, denoting $I_{kj}(t)$ the current flowing from node k to node j, we have for each k and at all time t

$$I_k(t) + \sum_{m \sim k} I_{mk}(t) = 0.$$

Then, with a_{mk} the complex conductance of line (m,k), we have $I_{mk}(t) = a_{mk}(V_m(t) - V_k(t))$ from which

$$V_k(t) \left(\sum_{m \sim k} a_{mk} \right) - \sum_{m \sim k} a_{mk} V_m(t) = I_k(t).$$

In vector form, this is

$$AV(t) = I(t) \tag{1}$$

with $A \in \mathbb{C}^{N \times N}$ defined as $A_{mk} = -a_{mk}$ for $m \sim k$ and $A_{kk} = \sum_{m \sim k} a_{mk}$.

We assume that $\bar{V} = \mathrm{E}[V(t)]$ is known empirically and therefore we know the relation $A\bar{V} = \bar{I}$. Subtracting this relation from (1), we obtain

$$Av(t) = i(t) \tag{2}$$

which is the voltage-current relation in normal situation. In practice, only an empirical approximation $\hat{V} \triangleq \frac{1}{n} \sum_{i=1}^n V(i)$ of $\bar{V}$ for n successive independent observations is known. In the following, we will consider test statistics based on the

[1] A more realistic model assumes $E[|i_k(t)|^2]$ different for each k. We keep $E[|i_k(t)|^2] = 1$ for readability of the derivations here.

sample covariance matrix of the n successive observations of $V(t)$ under the assumption that the system dimensions N and n are large. Under this assumption, it is asymptotically irrelevant whether $\tilde{V}$ or $\bar{V}$ is known, since the sample covariance matrices only differ from a rank-1 perturbation matrix with decreasing norm as $N, n \to \infty$. For simplicity of exposition, we assume that $\bar{V}$ is known, while simulation results will assume that only the estimate $\tilde{V}$ is known.

It is clear that A is of rank at most $(N-1)$ since all rows sum to zero. We may therefore project A on a subspace orthogonal to $\mathbf{1}\mathbf{1}^\mathsf{T}$ to ensure that the resulting matrix is invertible. Denote $U_A \in \mathbb{C}^{N\times(N-1)}$ a unitary matrix such that $A = U_A \Lambda_A U_A^*$ with $\Lambda_A \in \mathbb{C}^{(N-1)\times(N-1)}$ diagonal with positive entries. From (1), we then have $U_A^* A v(t) = \Lambda_A U_A^* v(t) = U_A^* i(t)$, Gaussian with zero mean and variance I_{N-1}. Therefore,

$$\mathrm{E}[U_A^* A v(t) v(t)^* A^* U_A] = \Lambda_A \mathrm{E}[U_A^* v(t) v(t)^* U_A] \Lambda_A = I_{N-1}$$

from which

$$\mathrm{E}[v'(t) v'(t)^*] = \Lambda_A^{-2}$$

where $v'(t) = U_A v(t)$ is a vector of independent components characterizing the network voltages.

II-B. Failure scenario: Hypothesis $\mathcal{H}_{(i,j)}$

Consider now the case of a partial or complete failure of line (i,j), which in our model translates as a sudden change in the value of a_{ij}. The objective is to derive the new distribution of $v'(t) = U_A^* v(t)$ under this condition. Note that A now becomes a matrix B (depending on i,j) defined by

$$\begin{aligned} B &= A + \bar{a}_{ij} e_i e_j^* + \bar{a}_{ij}^* e_j e_i^* - \bar{a}_{ij} e_i e_i^* - \bar{a}_{ij}^* e_j e_j^* \qquad (3) \\ &\triangleq A + C_{ij} \end{aligned}$$

where $a_{ij} - \bar{a}_{ij}$ is the new value of the parameter a_{ij} after failure ($\bar{a}_{ij} = a_{ij}$ in case of complete failure of line (i,j)), and the vector $e_i \in \mathbb{C}^N$ is defined as $e_i(i) = 1$ and $e_i(j) = 0$ for $j \neq i$. The matrix C_{ij} is therefore at most a rank-2 perturbation of A, whose image lies in the space $\mathrm{Span}(e_i, e_j)$.

In case of failure of line (i,j), we now have $Bv(t) = i(t) \sim \mathcal{CN}(0, I_N)$, where $\bar{V}$ is now evaluated on the basis of observations under failure of line (i,j). Since B also has its image in the subspace orthogonal to $\mathbf{1}\mathbf{1}^\mathsf{T}$, for any projector UU^* to this subspace, we can write $Bv(t) = BUU^* v(t)$, so in particular for $U = U_A$. We therefore have

$$U_A^* B U_A v'(t) \sim \mathcal{CN}(0, I_{N-1})$$

with $v'(t) = U_A v(t)$ and therefore

$$\mathrm{E}[v'(t) v'(t)^*] = (U_A^* B U_A)^{-2}.$$

We now observe that, between the non-failure and the failure scenarios, the covariance matrices $\mathrm{E}[v'(t)v'(t)^*]$ only differ by a rank-2 perturbation matrix.

The following section captures this behaviour and translates the failure detection and localization problems into the detection of a rank-2 perturbation matrix of the identity population covariance matrix, based on noisy sample observations.

II-C. Measurements

Let us now assume that, instead of the voltage $v(t)$ (or $v'(t)$), we have noisy observations

$$\begin{aligned} y(t) &= v(t) + \sigma w(t) \\ y'(t) &= v'(t) + \sigma w'(t) \end{aligned}$$

where $\sigma > 0$ and $w(t) \in \mathbb{C}^N$, $w'(t) \in \mathbb{C}^{N-1}$ are complex standard white Gaussian noise vectors.

From $B = A + C_{ij}$, we have

$$\begin{aligned} (U_A^* B U_A)^{-1} &= (U_A^*[A + C_{ij}]U_A)^{-1} \\ &= \Lambda_A^{-\frac{1}{2}} (I_{N-1} + \Lambda_A^{-\frac{1}{2}} U_A^* C_{ij} U_A \Lambda_A^{-\frac{1}{2}})^{-1} \Lambda_A^{-\frac{1}{2}}. \end{aligned}$$

We remind that $C_{ij} \in \mathbb{C}^{N\times N}$ has non-zero entries only in coordinates $(i,i),(i,j),(j,i)$ and (j,j). Isolating the submatrix $\bar{C}_{ij} \in \mathbb{C}^{2\times 2}$ extracted from C_{ij} for these coordinates, denoting $U_{A,ij}^*$ the matrix formed from the columns i and j of U_A^*, an application of Woodbury's identity gives

$$\begin{aligned} (U_A^* B U_A)^{-1} = \Lambda_A^{-\frac{1}{2}} (I_{N-1} &- \Lambda_A^{-\frac{1}{2}} U_{A,ij}^* \\ &\times [\bar{C}_{ij}^{-1} + U_{A,ij} \Lambda_A^{-1} U_{A,ij}^*]^{-1} U_{A,ij} \Lambda_A^{-\frac{1}{2}}) \Lambda_A^{-\frac{1}{2}}. \end{aligned}$$

This is clearly a rank-2 perturbation of Λ_A^{-1} with image lying in the image of $\Lambda_A^{-1} U_{A,ij}^*$. Taking the square of $(U_A^* B U_A)^{-1}$ leads to the conclusion that $(U_A^* B U_A)^{-2}$ is a rank-2 perturbation of Λ_A^{-2} with image lying in the image of $\Lambda_A^{-1} U_{A,ij}^*$. We then denote

$$(U_A^* B U_A)^{-2} = \Lambda_A^{-2} + C'_{ij}$$

for $C'_{ij} \in \mathbb{C}^{(N-1)\times(N-1)}$ a rank-2 matrix. Hence

$$\mathrm{E}[y(t) y(t)^*] = \Lambda_A^{-2} + C'_{ij} + \sigma^2 I_{N-1}.$$

Now, calling $R_A = \mathrm{E}[y(t)y(t)^*] = (U_A^* A U_A)^{-2} + \sigma^2 U_A^* U_A = \Lambda_A^{-2} + \sigma^2 I_{N-1}$, we have

$$\mathrm{E}[R_A^{-\frac{1}{2}} y'(t) y'^*(t) R_A^{-\frac{1}{2}}] = I_{N-1} + R_A^{-\frac{1}{2}} C'_{ij} R_A^{-\frac{1}{2}}$$

which is a rank-2 perturbation of I_{N-1} with image lying in the image of $R_A^{-\frac{1}{2}} \Lambda_A^{-1} U_{A,ij}^*$. From now on, we will consider

$$x(t) = R_A^{-\frac{1}{2}} y'(t)$$

as the vector of interest for the analysis, and consider the following state hypotheses:

$$\begin{cases} x(t) \sim \mathcal{CN}(0, I_{N-1}) & , \ (\mathcal{H}_0) \\ x(t) \sim \mathcal{CN}(0, I_{N-1} + P_{(i,j)}) & , \ (\mathcal{H}_{(i,j)}) \end{cases} \qquad (4)$$

where $P_{(i,j)} \triangleq R_A^{-\frac{1}{2}} C'_{ij} R_A^{-\frac{1}{2}}$.

The key observation is that a local failure, observed through the measurements of $v(t)$, translates into a small

perturbation in the covariance matrix of $x(t)$. If we observe infinitely many realizations of $x(t)$, then the hypothetical failures are characterized by the properties of the eigenspace associated with the two eigenvalues of the sample covariance matrix non equal to one. However, for fast detection, the number of observations of $x(t)$ must be small. The objective of the present article is then to provide line outage diagnostic algorithms based on finitely many observations of $x(t)$.

III. SUBSPACE FAILURE DIAGNOSTIC METHOD

Let us now consider here the hypothesis test (4) for generic matrices

$$P_{(i,j)} = \sum_{k=1}^{r} \omega_{ij,k} u_{ij,k} u_{ij,k}^*$$

of rank $r \ll N$ with $\omega_{ij,1} > \ldots > \omega_{ij,r}$ and $u_{ij,k}^* u_{ij,k'} = \delta_k^{k'}$. In contrast to the static scenario of [1], where single observations are sufficient to identify sudden changes in voltage phases, the natural fluctuations of $v(t)$ demand several observations $x(1), \ldots, x(n)$ of $x(t)$ to provide an efficient test statistic. Denoting $X = [x(1), \ldots, x(n)] \in \mathbb{C}^{N \times n}$, we wish to infer from X the most likely hypothesis among $\mathcal{H}_0$ and the hypotheses $\mathcal{H}_{(i,j)}$. However, for fast detection, it is also necessary for n not to be too large compared to N, making traditional $n \gg N$ tests impractical. In this work, we instead propose a subspace method based on the results of [4] on the asymptotic fluctuations of the largest eigenvalues of the *spiked* sample covariance matrix $\frac{1}{n} X X^*$ under hypothesis $\mathcal{H}_0$, as well as the recent work [3] on the asymptotic joint fluctuations of eigenvalues and eigenvector projections under hypothesis $\mathcal{H}_{(i,j)}$, as $N, n \to \infty$ and $N/n \to c > 0$. Similar to $P_{(i,j)}$, we write

$$\frac{1}{n} X X^* = \sum_{k=1}^{N} \lambda_k \hat{u}_k \hat{u}_k^*$$

with $\lambda_1 > \ldots > \lambda_N$ and $\hat{u}_k^* \hat{u}_{k'} = \delta_k^{k'}$.

We first recall the important results below. For simplicity, we only focus on the properties of the largest eigenvalues, which are most relevant in the context of electrical line outages.

III-A. Eigen-structure fluctuation

Under hypothesis $\mathcal{H}_0$, it is known that, as $N, n \to \infty$, $N/n \to c > 0$, the empirical eigenvalue distribution of $\frac{1}{n} X X^*$ converges weakly and almost surely to the Marčenko-Pastur law with support $[(1-\sqrt{c})^2, (1+\sqrt{c})^2]$ and that the extreme left and right eigenvalues converge almost surely to the edges of the support [2]. Moreover the largest eigenvalue of $\frac{1}{N} X X^*$ admits the following fluctuations:

Theorem 1: Denote

$$\lambda_1' \triangleq N^{\frac{2}{3}} \frac{\lambda_1 - (1+\sqrt{c})^2}{(1+\sqrt{c})^{\frac{4}{3}} c^{\frac{1}{2}}}.$$

where $c_N \triangleq N/n$. Then, $\lambda_1' \Rightarrow T_2$, as $N, n \to \infty$, $N/n \to c$, with T_2 the complex Tracy-Widom law [5].

In contrast, under $\mathcal{H}_{(i,j)}$, two situations arise:

- if $\omega_{ij,1} < \sqrt{c}$, then $\lambda_1 \xrightarrow{\text{a.s.}} (1+\sqrt{c})^2$ and $\lambda_1' \Rightarrow T_2$, with λ_1' defined in Theorem 1 [6].
- if $\omega_{ij,k} > \sqrt{c}$ for some k, then

$$\lambda_k \xrightarrow{\text{a.s.}} \rho_{ij,k} \triangleq 1 + \omega_{ij,k} + c(1+\omega_{ij,k})\omega_{ij,k}^{-1}$$
$$|\hat{u}_k^* u_{ij,k}|^2 \xrightarrow{\text{a.s.}} \xi_{ij,k} \triangleq (1 - c\omega_{ij,k}^{-2})(1 + c\omega_{ij,k}^{-1})^{-1}$$

the quantities above having the following fluctuations:
Theorem 2: Discarding the indexes ij for notational convenience, if $\omega_k > \sqrt{c}$, then

$$\sqrt{N} \begin{pmatrix} |u_k^* \hat{u}_k|^2 - \xi_k \\ \lambda_k - \rho_k \end{pmatrix} \Rightarrow \mathcal{N}(0, C_k)$$

where

$$C_k = \begin{bmatrix} \frac{c^2(1+\omega_k)^2}{(c+\omega_k)^2(\omega_k^2-c)} \left[\frac{c(1+\omega_k)^2}{(c+\omega_k)^2} + 1\right] & \frac{(1+\omega_k)^3 c^2}{(\omega_k+c)^2 \omega_k} \\ \frac{(1+\omega_k)^3 c^2}{(\omega_k+c)^2 \omega_k} & \frac{c(1+\omega_k)^2(\omega_k^2-c)}{\omega_k^2} \end{bmatrix}.$$

Also, $\sqrt{N} v^* \hat{u}_k \xrightarrow{\text{a.s.}} 0$, for $v \in \text{Span}(u_k^{\perp})$.
Under hypothesis $\mathcal{H}_{(ij)}$, C_k will be denoted $C_{ij,k}$.

III-B. Hypothesis testing

In the line outage detection context, the above results state that failures can be detected with high probability for large N, n if $\omega_{ij,1} > \sqrt{c_N}$ with $c_N \triangleq N/n$, and an *hypothesis rejection test* can be designed based on the fluctuations of λ_1 under $\mathcal{H}_0$.[2] Besides, once a failure is successfully detected, the fluctuations of the λ_k and $\hat{u}_k$, with k such that $\omega_{ij,k} > \sqrt{c}$ for all ij, allow to design an appropriate *hypothesis selection test* among all $\mathcal{H}_{(ij)}$. This is detailed in the following.

Given a maximally acceptable *false alarm rate* η (that is, the maximum probability for natural voltage fluctuations to be interpreted as failures), we have the following straightforward rejection test:

$$\lambda_1' \underset{\bar{\mathcal{H}}_0}{\overset{\mathcal{H}_0}{\lessgtr}} (T_2)^{-1}(1-\eta)$$

with $\lambda_1' = N^{\frac{2}{3}} \frac{\lambda_1 - (1+\sqrt{c})^2}{(1+\sqrt{c})^{\frac{4}{3}} c^{\frac{1}{2}}}$, where $\bar{\mathcal{H}}_0$ is the hypothesis of a system failure of any nature. Note that this test assumes large N, n and is therefore best suited for large systems.

Given the false alarm rate η, we may also evaluate the probability of acceptance of a failure of type $\mathcal{H}_{(ij)}$, i.e.

$$P\left(\lambda_1 > N^{-\frac{2}{3}} T_2^{-1}(1-\eta)(1+\sqrt{c_N})^{\frac{4}{3}} \sqrt{c_N} + (1+\sqrt{c_N})^2\right)$$

with $c_N \triangleq N/n$, which for large N, n is approximately

$$1 - \Phi(b_{ij}^{\eta}) \tag{5}$$

[2]The smallest eigenvalue $\omega_{ij,r}$ is very close to one in the outage line perturbation matrices, so that λ_N is not a relevant parameter for failure detection.

where b_{ij}^{η} is defined as

$$b_{ij}^{\eta} = \frac{N^{-\frac{2}{3}} T_2^{-1}(1-\eta)(1+\sqrt{c})^{\frac{4}{3}}\sqrt{c} + (1+\sqrt{c})^2 - \rho_{ij,1}}{N^{-\frac{1}{2}}\omega_{ij,1}^{-1}\sqrt{c}(1+\omega_{ij,1})(\omega_{ij,1}^2 - c)^{\frac{1}{2}}}$$

and Φ is the Gaussian distribution function.

If a positive decision in favor of $\mathcal{H}_0$ is taken, then, from Theorem 2, a natural test for deciding on the most likely hypothesis $\mathcal{H}_{(ij)}$ consists in selecting the index:

$$\arg\max_{(ij)\in S} - \begin{pmatrix} |u_{ij,1}^* \hat{u}_1|^2 - \xi_{ij,1} \\ \lambda_1 - \rho_{ij,1} \end{pmatrix}^{\mathsf{T}} C_{ij}^{-1} \begin{pmatrix} |u_{ij,1}^* \hat{u}_1|^2 - \xi_{ij,1} \\ \lambda_1 - \rho_{ij,1} \end{pmatrix} - \log\det C_{ij,1} \quad (6)$$

where S is the set of line indexes (i,j) such that $\omega_{ij,1} > \sqrt{c}$, and $C_{ij,k}$ is defined in Theorem 2.

IV. SIMULATIONS

In this section, we provide simulation results for the line outage diagnosis framework developed in Section IV applied to the IEEE-30 bus system. We consider a complete failure of line $(3,4)$, i.e. $\bar{a}_{ij} = a_{ij}$, which is in our framework one of the most difficult to identify since some other line failures show similar largest eigenvalues. The most difficult failure to detect altogether is a failure on line $(21,22)$, which requires n to be rather large compared to N for detectability. We consider that the observation noise has variance $\sigma^2 = -20$ dB.

In Figure 1, we show the theoretical and computed curves of the probability of correct detection of a complete failure on line $(3,4)$ for different target false alarm rates. In this scenario, a slight mismatch between the theory and the experiment appears, essentially due to the system size $N = 30$ which is not sufficient for large dimensional statistics to be accurate, especially in the tails of the underlying distributions, so in particular for small false alarm rates. In Figure 2, we depict the line failure detection and diagnosis performance under 10% false alarm rate, based on (6), which shows accurate performance of the localization test for not too large n.

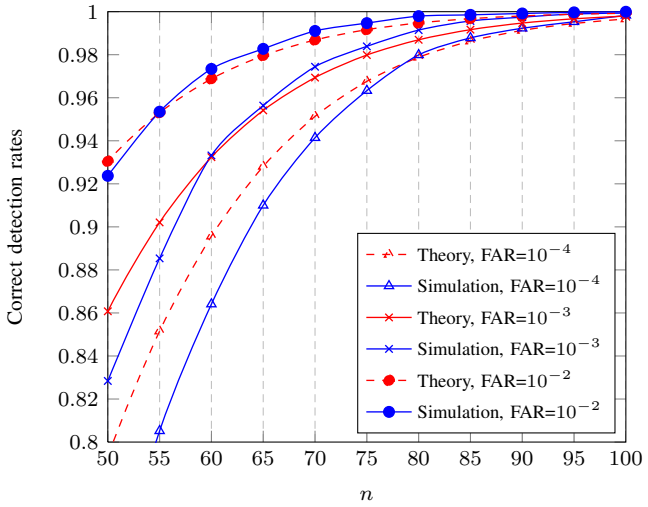

Fig. 1. Probability of detection of a complete failure on line $(3,4)$ in the IEEE-30 bus system. Comparison between theory and simulations.

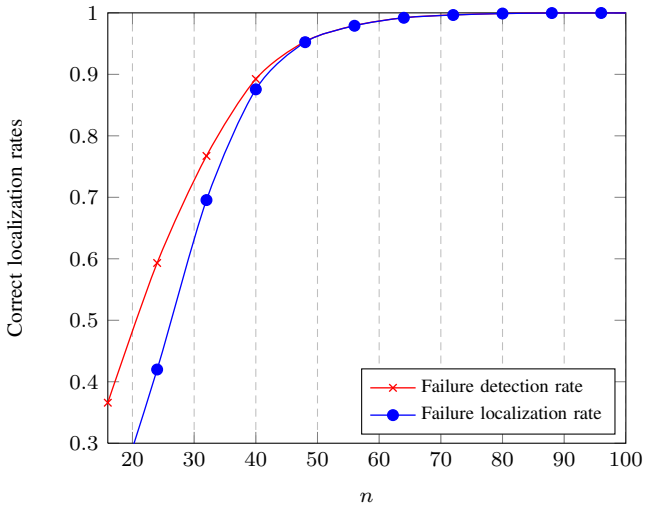

Fig. 2. Localization of a failure of line $(3,4)$ in the IEEE-30 bus system, for a 10% false alarm rate.

V. CONCLUSION

In this article, we applied a subspace method for line outage detection and localization in dynamical electricity networks based on frequent voltage measurements. This allows for a statistical treatment of failure diagnostics in fast varying electrical networks, therefore generalizing previous static methods.

VI. REFERENCES

[1] J. E. Tate and T. J. Overbye, "Line outage detection using phasor angle measurements," *Power Systems, IEEE Transactions on*, vol. 23, no. 4, pp. 1644–1652, 2008.

[2] R. Couillet and M. Debbah, *Random matrix methods for wireless communications*, 1st ed. New York, NY, USA: Cambridge University Press, 2011.

[3] R. Couillet and W. Hachem, "Local failure detection and diagnosis in large sensor networks," 2011.

[4] I. M. Johnstone, "On the distribution of the largest eigenvalue in principal components analysis," *Annals of Statistics*, vol. 99, no. 2, pp. 295–327, 2001.

[5] C. A. Tracy and H. Widom, "On orthogonal and symplectic matrix ensembles," *Communications in Mathematical Physics*, vol. 177, no. 3, pp. 727–754, 1996.

[6] J. Baik, G. Ben Arous, and S. Péché, "Phase transition of the largest eigenvalue for non-null complex sample covariance matrices," *The Annals of Probability*, vol. 33, no. 5, pp. 1643–1697, 2005.